

Original Article

Roles of vimentin and 14-3-3 zeta/delta in the inhibitory effects of heparin on PC-3M cell proliferation and B16-F10-luc-G5 cells metastasis

Yan PAN¹, Li-jun ZHONG², Hong ZHOU¹, Xin WANG¹, Kui CHEN¹, Hao-peng YANG¹, Yilixiati XIAOKAITI¹, Aikebaier MAIMAITI¹, Ling JIANG¹, Xue-jun LI^{1, *}

¹State Key Laboratory of Natural and Biomimetic Drugs, Department of Pharmacology, School of Basic Medical Sciences, Peking University and Institute of System Biomedicine, Peking University, Beijing 100191, China; ²Center of Medical Analysis, Peking University, Beijing 100191, China

Aim: To investigate the inhibitory effects of heparin on PC-3M cells proliferation *in vitro* and B16-F10-luc-G5 cells metastasis in Balb/c nude mice and identify the protein expression patterns to elucidate the action mechanism of heparin.

Methods: Human prostate cancer PC-3M cells were incubated with heparin 0.5 to 125 µg/mL for 24 h. The proliferation of PC-3M cells was assessed by MTS assay. BrdU incorporation and Ki67 expression were detected using a high content screening (HCS) assay. The cell cycle and apoptosis of PC-3M cells were tested by flow cytometry. B16-F10-luc-G5 carcinoma cells were injected into the lateral tail vein of 6-week old male Balb/c nude mice and heparin 30 mg/kg was administered iv 30 min before and 24 h after injection. The metasis of B16-F10-luc-G5 cells was detected by bioluminescence assay. Activated partial thromboplastin time (APTT) and hemorheological parameters were measured on d 14 after injection of B16-F10-luc-G5 carcinoma cells in Balb/c mice. The global protein changes in PC-3M cells and frozen lung tissues from mice burdened with B16-F10-luc-G5 cells were determined by 2-dimensional gel electrophoresis and image analysis. The protein expression of vimentin and 14-3-3 zeta/delta was measured by Western blot. The mRNA transcription of vimentin, transforming growth factor (TGF)-β, E-cadherin, and α_v-integrin was measured by RT-PCR.

Results: Heparin 25 and 125 µg/mL significantly inhibited the proliferation, arrested the cells in G₁ phase, and suppressed BrdU incorporation and Ki67 expression in PC-3M cells compared with the model group. But it had no significant effect on apoptosis of PC-3M cells. Heparin 30 mg/kg markedly inhibits the metastasis of B16-F10-luc-G5 cells on day 8. Additionally, heparin administration maintained relatively normal red blood hematocrit but had no influence on APTT in nude mice burdened with B16-F10-luc-G5 cells. Thirty of down-regulated protein spots were identified after heparin treatment, many of which are related to tumor development, extracellular signaling, energy metabolism, and cellular proliferation. Vimentin and 14-3-3 zeta/delta were identified in common in PC-3M cells and the lungs of mice bearing B16-F10-luc-G5 carcinoma cells. Heparin 25 and 125 µg/mL decreased the protein expression of vimentin and 14-3-3 zeta/delta and the mRNA expression of α_v-integrin. Heparin 125 µg/mL decreased *vimentin* and *E-cadherin* mRNA transcription while increased *TGF-β* mRNA transcription in the PC-3M cells, but the differences were not significant. Transfection of vimentin-targeted siRNA for 48 h significantly decreased the BrdU incorporation and Ki67 expression in PC-3M cells.

Conclusion: Heparin inhibited PC-3M cell proliferation *in vitro* and B16-F10-luc-G5 cells metastasis in nude mice by inhibition of vimentin, 14-3-3 zeta/delta, and α_v-integrin expression.

Keywords: heparin; cell growth; proteome; vimentin; 14-3-3 zeta/delta; α_v-integrin

Acta Pharmacologica Sinica (2012) 33: 798–808; doi: 10.1038/aps.2012.42

Introduction

Despite the progress made over decades of research, cancer remains a major threat to human health with significant morbidity and mortality. In the development of new anti-

tumor treatments, multi-targeting drugs continue to emerge as investigators search for candidates among currently available agents. Drugs with a long history of safe clinical use are especially attractive for testing their efficacy against cancer, which may be outside of the scope of their original application. In addition to its anti-coagulant activity, heparin is known to have suppressive effects on multiple biologic functions, such as hypertension^[1], inflammation^[2], and cellular proliferation^[3].

* To whom correspondence should be addressed.

E-mail xjli@bjmu.edu.cn

Received 2012-02-14 Accepted 2012-03-30

Heparin is a polysulfated glycosaminoglycan with a highly negative charge. Two trials (FAMOUS and MALT) previously studied the effect of unfractionated heparin (UFH)^[4] or low molecular weight heparin (LMWH)^[5] in patients with small cell lung cancer. In both of these studies, a statistically significant survival advantage was observed in patients randomized to chemotherapy plus UFH or LMWH relative to patients who received chemotherapy alone. While several clinical studies strongly support an anti-cancer activity of heparin, especially LMWH, many questions remain unresolved^[6]. For example, it is still unknown whether and how heparin modulates survival of carcinoma cells, although a number of biological properties have been postulated to explain the effects of heparin on the malignant process.

In this investigation, we addressed the potential inhibitory effects of heparin on growth of human prostate cancer cells (PC-3M) and metastasis of B16-F10-luc-G5 carcinoma cells in Balb/c nude mice with single dose and twice injection way and monitoring with living imaging technology. For the spontaneous hemorrhage is the main side effects of heparin, we also evaluated the systemic bleeding parameters of activated partial thromboplastin time (APTT) and hemorheological parameters of whole blood viscosity, elongation index (EI), orientation index (OI) and hematocrit of red blood cells, which are related greatly with tumor metastasis. By using a proteomic approach, we also identified proteins significantly associated with the anti-tumor and anti-metastatic effects of heparin to explore its new molecular mechanisms.

Materials and methods

Materials

DMEM medium, fetal bovine serum (FBS), penicillin and streptomycin were purchased from GIBCO (Grand Island, NY, USA). BrdU and Ki67 Cell Proliferation Kit for high content screening (HCS) was from Cellomics, Inc (Pittsburgh, PA, USA). B16-F10-Luc-G5 was from Caliper Life Sciences (Hopkinton, MA, USA). The vimentin specific antibody was from Beijing Biosynthesis Biotechnology (Beijing, China). Heparin sodium salt from porcine intestinal mucosa was purchased from Sigma-Aldrich, Inc (Saint Louis, MO, USA).

Cell culture

PC-3M cells were cultured in DMEM medium containing 10% heat-inactivated FBS, 100 U/mL penicillin and 100 µg/mL streptomycin in a humidified incubator with 5% CO₂ in air at 37 °C. B16-F10-Luc-G5 cells were cultured in DMEM medium containing 10% heat-inactivated FBS, 100 U/mL penicillin and 100 µg/mL streptomycin in a humidified incubator with 5% CO₂ in air at 37 °C.

Cell proliferation

PC-3M cells were cultured in 96-well plates. When the cells reached approximately 70% confluency, different doses of heparin (0, 0.5, 1, 5, 25, and 125 µg/mL) were added to the culture and incubated for 24 h. Every group has six wells. Each independent experiment was performed three times. MTS

assays were then conducted using the CellTiter96 Aqueous Non-Radioactive Cell Proliferation Assay kit (Promega Corp, Madison, WI, USA), according to the manufacturer's instructions. Absorbance was measured at a wavelength of 490 nm, and the absorbance values of treated cells were calculated as a percentage of the absorbance of untreated cells.

Cell cycle and apoptosis analysis

For flow cytometric analysis of DNA content, heparin was added to PC-3M cells in the mid-logarithmic phase. After 24 h, cells were collected, pelleted, washed with phosphate-buffered saline (PBS) and resuspended in PBS containing 20 mg/L propidium iodide (PI, Sigma, St Louis, MO, USA) and 1 g/L ribonuclease A (RNAase A). Fixed cells for each experimental condition were examined by flow cytometry.

For analysis of apoptosis after incubation with heparin for 24 h, PC-3M cells (1×10⁶ cells per treatment condition) were fixed and stained with 5 mL Annexin V-FITC (BD PharMingen, San Diego, CA) and 5 mL PI. Flow cytometric analysis was performed on 1×10⁴ cells per sample and analyzed using a FACS Calibur (Becton Dickinson, Franklin Lakes, NJ) with a single laser emitting excitation light at 488 nm.

Multiparametric proliferation assay with a HCS analyzer

The 5-bromo-2'-deoxyuridine (BrdU) and Ki67 Cell Proliferation Kit for HCS reagent kit was used for simultaneous quantification of DNA replication and Ki67 proliferation marker in the same cell. It allows direct measurements of BrdU incorporation and Ki67 expression using a fixed end-point assay based on immunofluorescence detection in cells grown on standard high-density microplates. The primary antibodies were directed toward BrdU and Ki67 (mouse monoclonal and rabbit polyclonal antibodies, respectively) and secondary antibodies were conjugated with DyLight Fluor 488 (green) and DyLight Fluor 549 (orange). Cells were stained and fixed, and total cells per well of the microplates were analyzed using an ArrayScan HCS system (Cellomics Inc., Pittsburgh, PA, USA).

In vivo metastasis

B16-F10-luc-G5 cells that had been engineered to stably express firefly luciferase (Xenogen Corporation, Alameda, CA, USA) were injected into the lateral tail vein (5×10⁶ cells/100 µL/mouse) of 6-week-old BALB/c nude mice. Mice were anesthetized and given 150 mg/g of D-luciferin in PBS by intraperitoneal injection. Bioluminescence was imaged with a charge-coupled device camera (IVIS; Xenogen) at 10 min after injection. Mice were anesthetized using 1%–3% isoflurane (Abbott Laboratories, Chicago, IL, USA). Bioluminescence from relative optical intensity was defined manually, and data were expressed as photon flux normalized to background photon flux, which was defined from relative optical intensity obtained from a control mouse not injected with luciferin. Animal handling and procedures were approved by the Peking University Health Science Center Institutional Animal Care and Use Committee. All animal studies conformed to the principles outlined in the Declaration of Helsinki.

Activated partial thromboplastin time (APTT) and hemorheological measurements

On day 14, blood specimens of BALB/c nude mice injected with B16-F10-luc-G5 cells were collected by retro-orbital bleeding after anesthesia with ether. Anesthesia was achieved by placing the mouse in a container containing cotton wool soaked in ether. The anesthetic plane was assessed by pinching the toe, tail or ear of the animal. The respiration rate was even and the color of the mucus membranes was bright pink. As the blood was collected, there was no evidence of pain observed in the animals. Whole blood with sodium citrate anticoagulant (9:1), centrifuged at 3000 r/min for 10 min, and upper plasma was used to detect APTT. APTT was measured in 50 μ L plasma using C2000-4 Type Coagulometer (Beijing Precil Instrument Co, Ltd). Whole blood with sodium citrate anticoagulant was used for hemorheological measurements. Whole blood viscosity was detected in 800 μ L of blood by using a viscosity meter (LBY-N6C, Precil Group, Beijing, China). Red blood cell deformability was determined by measuring the elongation index (EI) and orientation index (OI) using an ektacytometer (LBY-BX2 Precil Group, Beijing, China). Blood samples diluted with polyvinyl pyrrolidone (PVP) were added to the base plate of the instrument. The EI and OI values were measured under stress rates of 100/s and 1000/s. Hematocrit of red blood cells was measured by aspirating blood into a capillary tube, sealing off the end of the tube and then centrifuging it at 10000 r/min for 5 min. The height of the red blood cells deposited at the bottom end of the tube was recorded.

Two-dimensional gel electrophoresis (2-DE) and image analysis

Monolayers of PC-3M cells were treated with or without heparin (125 μ g/mL) for 24 h. Cells were harvested using homemade scrapers. The resulting pellets were resuspended in 100 mL of solubilization buffer containing 40 mmol/L Tris, 8 mol/L urea, 4% *w/v* CHAPS, 60 mmol/L DTT and 1 mmol/L PMSF. After three freeze-thaw cycles, samples were centrifuged at 17000 \times *g* for 15 min, and the supernatants were collected. Another pair of samples tested were the frozen mice lung tissues, which were thawed at room temperature before total proteins were extracted as mentioned above and the protein concentration measured by the Bradford method. First dimension isoelectric focusing (IEF) was performed using linear immobilized pH gradient readystrips (24 cm, pH 3–10, Bio-Rad Laboratories, Inc, Hercules, CA, USA). Protein samples (500 μ g) from each group were solubilized in rehydration buffer [8 mol/L urea, 4% CHAPS, 65 mmol/L DTT, 0.2% Bio-Lyte (Bio-Rad) and 0.001% bromothymol blue] to a volume of 125 mL and allowed to incubate at room temperature for 30 min. After positive rehydration for 12 h at 50 V, IEF was run at 20°C in the following steps: 250 V linear for 30 min, 500 V rapid for 30 min, 4000 V linear for 3 h, 4000 V rapid until 20000 V. The IEF strips were then equilibrated by serial incubation (15 min) in equilibration buffer (6 mol/L urea, 2% SDS, 0.375 mol/L Tris-HCl at pH 8.8, 20% glycerol and 20 mg/mL DTT) and in equilibration buffer containing 2.5% iodoacet-

amide instead of DTT. Subsequently, the samples were separated in the second dimension on 12% polyacrylamide gels at 80 V for 10 min and then at 110 V for 50–60 min. Gels were stained with Coomassie Blue. The differentially expressed protein spots were excised manually from the sodium dodecyl sulphate-polyacrylamide gel (SDS-PAGE) and subjected to in-gel tryptic digestion.

Mass spectrometry identification of proteins

Proteins of interest were analyzed by nanoelectrospray with a hybrid quadrupole time-of-flight (Q-TOF) mass spectrometer (Waters, Milford, MA, USA). The peptide mixture was carried out on a Waters Capillary liquid chromatography system including three pumps, A, B, and C (Waters). Fused silica tubing were packed with Symmetry 300™ C18, 3.5 mm spherical particles with a pore diameter of 1008 (Waters). The flow rate was set at 2.5 mL/min. Samples were injected at a flow rate of 20 mL/min.

Western blot analysis

Equal amounts of protein were analyzed by SDS-PAGE on a 10% polyacrylamide gel for vimentin and 14-3-3 zeta/delta and transferred to a polyvinylidene difluoride membrane (Millipore Corp, Bedford, MA, USA). The membrane with blotted proteins was blocked for 1 h with blocking buffer containing 5% non-fat dry milk and 0.05% Tween 20 in Tris-buffered saline (TBS-T), followed by incubation with vimentin antibody diluted (1:100) in blocking buffer overnight at 4°C. The membrane was then washed three times with TBS-T for 30 min and incubated at room temperature for 1 h with diluted (1:2000) secondary AP-labeled IgG (Santa Cruz Biotechnology, Santa Cruz, CA, USA). Blots were extensively washed in TBST buffer and detection was done using the NBT/BCIP reaction (Amersco, NJ, USA)^[7].

Ribonucleic acid isolation and reverse transcription-polymerase chain reaction (RT-PCR)

Total RNA was isolated using Trizol reagent (Invitrogen, Groningen, the Netherlands). First-strand cDNAs were generated from RNA samples by reverse transcription using oligo (dT). The following primers were used to amplify fragments of *β -actin*: 5'-ATCATGTTTGAGACCTTCAACA-3' (sense) and 5'-CATCTCTTGCTCGAAGTCCA-3' (antisense); transforming growth factor (*TGF*)- β : 5'-CAAGTGGACATCAAC GGTGAGG-3' (sense) and 5'-TGGC-CATGAGAAGCAGGAAAGG-3' (antisense); *vimentin*: 5'-GACAATGCGTCTCTGGCACGTCTT-3' (sense) and 5'-TCCTCCGCCCTCCTGCAGGTTCTT-3' (antisense); *α_v -integrin*: 5'-GACTGTGTGGAAGACAATGTCTGTAAACCC-3' (sense) and 5'-CCAGCTAAGAGTTGAGTTCCAGCC-3' (antisense); *E-cadherin*: 5'-TGGAGGAATTCTTGCTTTGC-3' (sense) and 5'-CGTACATGTCAGCCAGCTTC-3' (antisense).

Short interfering ribonucleic acid (siRNA) transfection

siRNA duplexes used in this study were bought from Santa Cruz, to interfere with vimentin expression. Non-silencing

siRNA (5'-UUAAGUAGCUUGGCCUUGATdT-3' and 5'-UCAAGGCCAAGCUACUUAATdT-3') was used as the negative controls. siRNA duplexes were transfected into HUVECs with siRNA transfection reagent (Polyplus-transfection Inc, San Marcos, CA, USA), according to the manufacturer's instructions. After transfection for 48 h, cells were subjected to multiparametric proliferation assay with a HCS analyzer.

Statistical analysis

Data were expressed as means±standard error of mean (SEM). Statistical significance of differences between means was determined by one-way analysis of variance (ANOVA) followed by Dunnett's test (Graphpad Prism 5 software). $P < 0.05$ was considered to be statistically significant.

Results

Effect of heparin on PC-3M cell viability and cell cycle

As estimated by the MTS assay, cell viability decreased dose dependently after 24 h of exposure to heparin at different concentrations (0.5, 1, 5, 25, and 125 $\mu\text{g}/\text{mL}$) (Figure 1A). Heparin 5, 25, and 125 $\mu\text{g}/\text{mL}$ arrested cells in the G_1 phase and influence DNA synthesis, with a significant effect at 125 $\mu\text{g}/\text{mL}$ ($P < 0.05$, Figure 1B). Correspondingly, cells in the S phase decreased with increasing doses of heparin.

Effect of heparin on apoptosis of PC-3M cells

Annexin V⁺ and PI⁻ staining represented early apoptotic cells, and Annexin V⁺ and PI⁺ staining represented late apoptotic and necrotic cells. Although the apoptotic cells were slightly elevated in the 125 $\mu\text{g}/\text{mL}$ heparin treated group compared with the vehicle treated group, the difference was not significant (control: 1.55%±0.19% vs 5 $\mu\text{g}/\text{mL}$ heparin: 1.44%±0.06%, 25 $\mu\text{g}/\text{mL}$ heparin: 2.21%±0.08%, 125 $\mu\text{g}/\text{mL}$ heparin: 5.91%±0.15%) (Figure 1C).

Effect of heparin on BrdU incorporation and Ki67 expression in PC-3M cells

BrdU incorporation and Ki67 activation in PC-3M cells were measured simultaneously in the same cells as described in Methods. As an alternative to [³H]thymidine, BrdU, a thymidine analog, enables detection of DNA replication in actively proliferating cells using a monoclonal antibody directed against BrdU and fluorophore-conjugated secondary antibody. In addition, Ki67 antigen-positive cells can provide a specific and accurate indication of proliferating cells. As determined

by HCS, we found that heparin suppressed BrdU incorporation and Ki67 expression in PC-3M cells compared to the control group, with statistically significant differences seen at the dosage of 125 $\mu\text{g}/\text{mL}$ (Figure 1D).

Heparin inhibits B16-F10-luc-G5 cell lung metastasis in Balb/c nude mice

Balb/c nude mice were implanted with B16-F10-luc-G5 carcinoma cells by tail vein injection and systemically treated with vehicle (model), 30 mg/kg heparin intravenously 30 min before B16-F10-luc-G5 carcinoma cell injection and 24 h after B16-F10-luc-G5 carcinoma cell injection. From day 2, the growth of B16-F10-luc-G5 tumor burden over time in representative Balb/c nude mice was measured by *in vivo* imaging. By this analysis, progression of tumors in the whole body of mice and lung tissue was delayed and reduced in the 30 mg/kg heparin treatment group, and the growth of the primary tumor was reduced significantly from day 8 onward when detected from the ventral (A, B, C) and dorsal (D, E, F) views ($P < 0.01$, Figure 2).

Heparin influences APTT and hemorheological parameters of Balb/c nude mice burdened with B16-F10-luc-G5 cells

At the 100/s and 1000/s shear rate, heparin could obviously decrease the whole blood viscosity, and there were significant differences when the tumor burdened (model) group was compared with the normal group or the heparin treated group ($P < 0.01$, Table 1). Factors influencing whole blood viscosity were measured including red blood hematocrit, EI and OI. We also found that in the model group, red blood hematocrit, EI and OI were decreased significantly compared with the normal group ($P < 0.01$) at the 100/s shear rate. At the shear rate of 1000/s in the model group, OI was decreased significantly compared with the normal group ($P < 0.01$), but no significant difference was detected for EI. Additionally, heparin maintained relatively normal red blood hematocrit, with EI and OI at the 100/s shear rate and OI at the 1000/s shear rate being significantly different with the model group ($P < 0.01$, Table 1). We had not found the difference in APTT between normal Balb/c nude mice with those burdened with B16-F10-luc-G5 cells; and heparin had also no influence on APTT of Balb/c nude mice burdened with B16-F10-luc-G5 cells.

Comparative proteomic analysis of PC-3M cells with or without heparin treatment

To explore the molecular mechanisms by which heparin exerts

Table 1. Effect of heparin on activated partial thromboplastin time (APTT) and hemorheological parameters in Balb/c nude mice burdened with B16-F10-luc-G5 cells. Mean±SEM. $n=5$. ^c $P < 0.01$ vs model.

Drug	Hematocrit (%)	Elongation Index		Orientation Index		Whole blood viscosity (mPa/s)		APTT (s)
		100/s	1000/s	100/s	1000/s	100/s	1000/s	
Normal	39±3.99 ^c	36.61±5.58 ^c	66.9±4.16	8.2±0.74 ^c	10.1±1.15 ^c	7.77±0.64 ^c	3.54±0.47 ^c	28.6±4.35
Model	21±4.60	28.2±2.69	64.2±3.58	4.94±0.69	5.03±0.24	12.19±2.28	4.58±0.02	27.11±3.13
Heparin	44±4.55 ^c	37.6±4.60 ^c	65.6±4.80	8.54±0.83 ^c	9.34±0.91 ^c	8.06±0.13 ^c	3.88±0.11 ^c	29.02±4.08

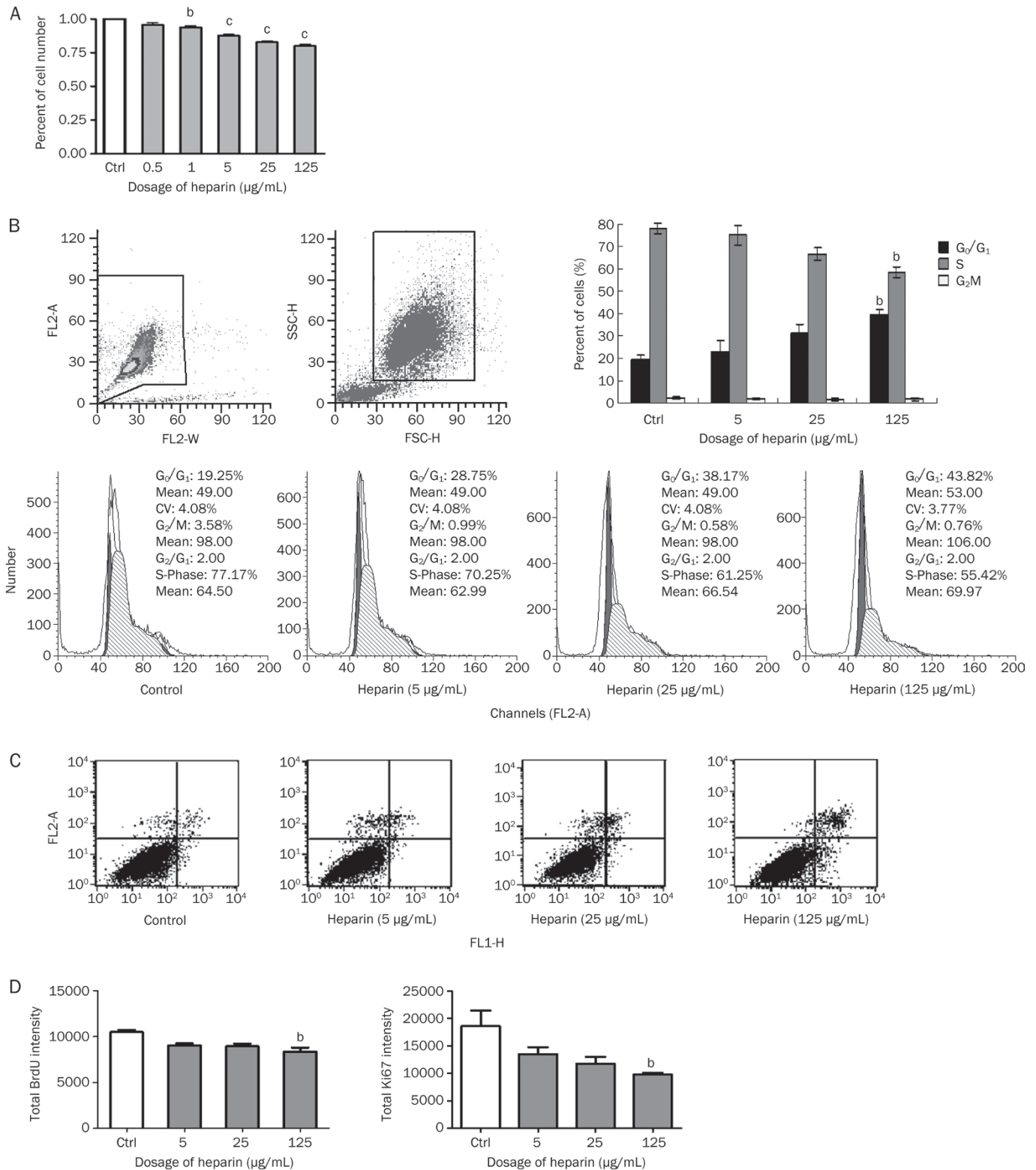


Figure 1. Heparin inhibits PC-3M cell growth. (A) MTS assays demonstrated a heparin-induced, dose-dependent decrease in PC-3M cell growth. (B) Flow cytometry showed that heparin treatment (5, 25, and 125 µg/mL, 24 h) resulted in marked cell cycle changes. (C) Flow cytometric analysis by Annexin V and PI double staining showed that heparin treatment (5, 25, and 125 µg/mL, 24 h) induced mild cell apoptosis. (D) HCS analysis showed that heparin suppressed BrdU incorporation and Ki67 expression in PC-3M cells. A total of 3000 cells were plated per well and incubated for 24 h before treatment with 5, 25, and 125 µg/mL heparin for 24 h. Control wells were treated with PBS per well. BrdU incorporation and Ki67 expression were measured simultaneously. Mean±SEM. $n=6$. ^b $P<0.05$, ^c $P<0.01$ compared with control. Each independent experiment was performed three times.

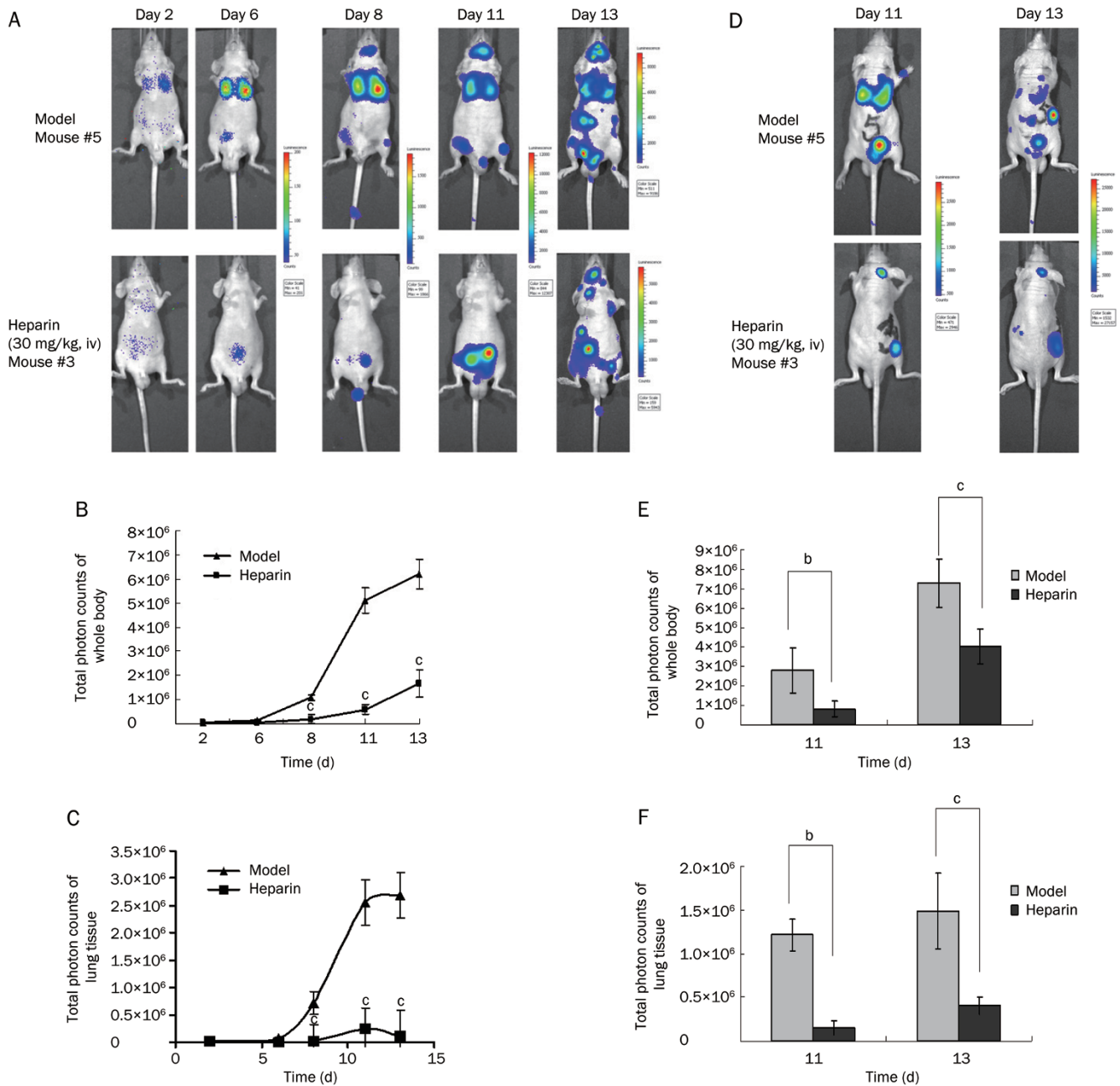


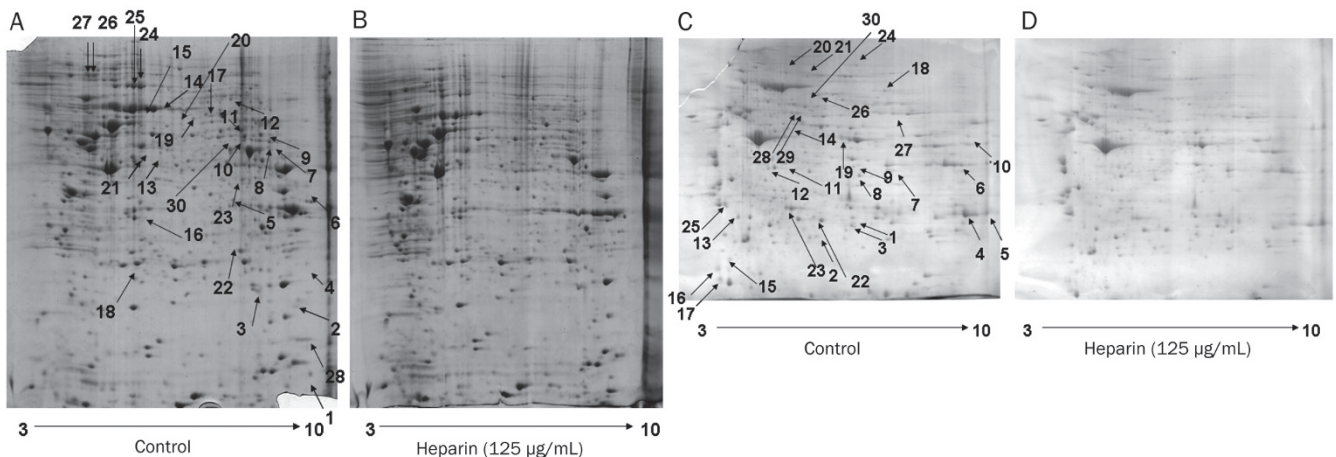
Figure 2. *In vivo* imaging of B16-F10-luc-G5 cell-derived tumors in mice. The cells (5×10^6) were injected intravenously through the tail vein of male BALB/c nude mice. Mice were imaged *in vivo* from the ventral (A) and dorsal (D) views between 2 to 14 days after the injection. Shown are images of one representative control (saline) animal and one representative heparin-treated mouse. Images were set on a pseudocolor scale to show relative bioluminescent changes over time. Metastatic signals reappeared on the day following administration of control mice with vehicle and multiple signals developed on day 6. *In vivo* imaging confirmed metastases in lungs (highest signal), ileum, jaws and skin (lower signal). Mice administered heparin (30 mg/kg, 30 min before and 24 h after tumor cell injection via the tail vein) showed significant reduction of pulmonary metastatic nodules. B, C, E, F show the statistical analysis of the total photon counts of whole body (B, E) or lung tissue (C, F) of BALB/c nude mice burdened with B16-F10-luc-G5 cells from the ventral (B, C) and dorsal (E, F) views. Mean \pm SEM. $n=3$. ^b $P < 0.05$, ^c $P < 0.01$ compared with the vehicle-treated control group.

anti-tumor and anti-proliferative effects in PC-3M cells, we compared the protein expression patterns in heparin treated (125 μ g/mL) and untreated cells. 2-DE analysis showed generally similar protein expression patterns in the heparin treated and untreated PC-3M cells (Figure 3A, B). The protein

spots were analyzed by PDQuest software, and 83 protein spots were significantly decreased in heparin treated versus untreated PC-3M cells ($P < 0.05$, Supporting information). Thirty of these obviously decreased spots after heparin treatment were identified by Q-TOF analysis (Table 2).

Table 2. Thirty of the significantly decreased spots after heparin treatment in PC-3M cells identified by Q-TOF analysis and search of the Mascot database.

Protein spot	Protein name	Mass	Score	Matches	Sequences	emPAI
1	Anterior gradient protein 2 (AGR2)	20 024	497	27 (17)	8 (6)	3.06
2	Adenylate kinase isoenzyme 1 (KAD1)	21 735	190	9 (5)	6 (5)	1
3	GTP-binding nuclear protein Ran (RAN)	24 579	694	29 (24)	12 (10)	3.63
4	14-3-3 protein zeta/delta 1433Z_HUMAN	27 899	89	1 (1)	1 (1)	0.12
5	Heterogeneous nuclear ribonucleoprotein D0 (HNRPD_HUMAN)	38 581	65	2 (2)	1 (1)	0.09
6	Heterogeneous nuclear ribonucleoprotein A3 (ROA3_HUMAN)	39 799	170	6 (5)	4 (3)	0.14
7	ATP synthase subunit alpha, mitochondrial (ATPA_HUMAN)	59 828	240	24 (13)	13 (8)	0.53
8	ATP synthase subunit alpha, mitochondrial ATPA_HUMAN	59 828	29	2 (1)	2 (1)	0.98
9	Annexin A11ANX11_HUMAN	54 697	724	19 (16)	8 (7)	0.57
10	Vimentin	55 123	1 124	51 (29)	21 (14)	1.84
11	Dihydrolipoyl dehydrogenase, mitochondrial DLDH_HUMAN	54 713	283	12 (10)	6 (4)	1.23
12	Prelamin-A/C LMNA_HUMAN	74 380	1 332	45 (38)	27 (22)	1.11
13	Dihydrolipoyllysine-residue succinyltransferase component of 2-ox oglutarate dehydrogenase complex, mitochondrial ODO2_HUMAN	49 067	225	6 (4)	4 (2)	0.91
14	Stress-70 protein, mitochondrial GRP75_HUMAN	73 920	163	5 (4)	5 (4)	0.08
15	Stress-70 protein, mitochondrial GRP75_HUMAN	73 920	149	3 (3)	2 (2)	0.09
16	L-lactate dehydrogenase B chain LDHB_HUMAN	36 900	193	6 (5)	5 (4)	0.46
17	T-complex protein 1 subunit zeta TCPZ_HUMAN	58 444	343	12 (9)	5 (4)	0.39
18	Heat shock protein beta-1 HSPB1_HUMAN	22 826	1 172	36 (27)	12 (10)	4.91
19	T-complex protein 1 subunit gamma TCPG_HUMAN	61 066	103	4 (3)	3 (2)	1.55
20	Pyruvate kinase isozymes M1/M2 KPVM_HUMAN	58 470	88	3 (2)	3 (2)	1.21
21	RuvB-like 2 RUVB2_HUMAN	51 296	262	9 (7)	6 (5)	0.45
22	Phosphoglycerate mutase 1 PGAM1_HUMAN	28 900	420	17 (11)	7 (7)	1.67
23	Elongation factor Tu, mitochondrial EFTU_HUMAN	49 852	1 519	42 (31)	15 (11)	1.79
24	Heat shock protein HSP 90-alpha HS90A_HUMAN	85 006	1 345	41 (31)	26 (20)	1.48
25	Heat shock protein 75 kDa, mitochondrial TRAP1_HUMAN	80 345	285	4 (4)	1 (1)	0.04
26	Heat shock protein HSP 90-beta HS90B_HUMAN	83 554	352	7 (5)	3 (2)	0.12
27	Endoplasmic ENPL_HUMAN	92 696	139	3 (2)	3 (2)	0.11
28	Peptidyl-prolyl <i>cis-trans</i> isomerase F, mitochondrial PPIF_HUMAN	22 368	288	9 (5)	7 (4)	0.67
29	Beta-enolase ENOA_HUMAN	47 481	3 394	86 (64)	29 (21)	6.49
30	Voltage-dependent anion-selective channel protein 1 VDAC1_HUMAN	30 868	1 502	40 (33)	13 (11)	2.78

**Figure 3.** 2-DE analysis of protein expression in PC-3M cells and lungs of mice burdened with B16-F10-luc-G5 cells with or without heparin treatment. Representative 2-DE maps of proteins in PC-3M cell lysis without (A) or with heparin treatment (B). Representative 2-DE maps of proteins in lysed lung tissues of mice bearing B16-F10-luc-G5 cells without (C) or with (D) heparin administration. Approximately 500 μg of total protein were focused on linear immobilized pH gradient strips (pH 3–10, 24 cm) before separating on a 12% sodium dodecyl sulphate–polyacrylamide gel and staining with Coomassie blue for detecting protein spots. The experiment was performed three times.

Comparative proteomic analysis of lungs of mice bearing B16-F10-luc-G5 cells with or without heparin administration

To further elucidate the possible novel molecular mechanisms by which heparin might exert its anti-tumor and anti-metastatic effects in Balb/c nude mice burdened with B16-F10-luc-G5 cells, we compared protein expression patterns in the lungs of heparin-treated and untreated (control) mice. 2-DE analysis showed generally similar protein expression patterns in the heparin-treated and untreated groups (Figure 3C and 3D). Among them, 30 obviously different spots (indicated by arrows) were identified by using Q-TOF analysis (Table 3).

Effect of heparin on expression levels of 14-3-3 zeta/delta, vimentin, E-cadherin, TGF- β , and α_v -integrin in PC-3M cells

After comparing the 2-DE results from PC-3M cells and lungs of mice burdened with B16-F10-luc-G5 cells, we found 14-3-3 zeta/delta and vimentin protein spots were identified in common. Then, our Western blot analysis confirmed that heparin could dose-dependently decrease the protein expression of 14-3-3 zeta/delta and vimentin, and there were significant differences at 25 and 125 $\mu\text{g}/\text{mL}$ (Figure 4A). Cytoskeleton

protein vimentin is involved in tumor mobility, adhesion, and epithelial to mesenchymal transition (EMT). Vimentin also co-localizes with $\alpha_v\beta_3$ -integrin (focal contacts) when tumor cell moved and thought as an important marker of tumor cell EMT, along with E-cadherin, TGF- β . To determine whether E-cadherin, TGF- β and α_v -integrin are transcriptionally regulated by heparin, RT-PCR analysis was performed on heparin treated PC-3M cells. *Vimentin* and *E-cadherin* mRNA decreased at the high dosage of heparin, while *TGF- β* mRNA increased with heparin treatment in the PC-3M cells (Figure 4B), although the differences were not significant. Expression of *α_v -integrin* mRNA in PC-3M cells decreased with heparin 25 and 125 $\mu\text{g}/\text{mL}$ treatment (Figure 4C).

The effect of vimentin-targetted siRNA on PC-3M cell proliferation

When PC-3M cells were transfected with siRNA against the vimentin gene for 48 h, the expression of vimentin in cells was partially reduced by 35% in comparison to the controls ($P < 0.05$; Figure 5A) and the BrdU incorporation and Ki67 activation in PC-3M cells was reduced significantly compared with the control ($P < 0.05$; Figure 5B).

Table 3. Thirty of the significantly decreased spots after heparin administration in lung tissue of Balb/c nude mice burdened with B16-F10-luc-G5 cells identified by Q-TOF analysis and search of the Mascot database.

Protein spot	Protein name	Mass	Score	Matches	Sequences	emPAI
1	Carbonyl reductase [NADPH]	26 056	335	15 (9)	7 (5)	1.32
2	14-3-3 protein zeta/delta	27 925	370	15 (11)	10 (7)	2.08
3	Hemoglobin subunit beta-1	15 944	79	1 (1)	1 (1)	0.21
4	Selenium-binding protein 1	53 051	72	4 (3)	3 (2)	0.13
5	Elongation factor 1-beta	24 849	344	5 (4)	3 (3)	0.46
6	Phosphoglycerate mutase 2	28 980	350	29 (21)	10 (8)	2.31
7	Carbonyl reductase [NADPH] 2	26 056	662	34 (23)	12 (7)	1.96
8	Troponin I, fast skeletal muscle	21 515	268	26 (15)	9 (5)	2.68
9	Hemoglobin subunit alpha	15 133	165	6 (6)	3 (3)	0.84
10	Carbonic anhydrase 3	29 633	144	31 (11)	8 (5)	1.34
11	Triosephosphate isomerase	32 684	65	25 (7)	10 (4)	0.47
12	Transcription factor BTF3	22 017	34	9 (1)	4 (1)	0.33
13	HIV Tat-specific factor 1 homolog	86 644	27	1 (0)	1 (0)	0.04
14	Transgelin	22 618	19	4 (0)	3 (0)	0.15
15	Filamin A-interacting protein 1-like	130 263	15	2 (0)	1 (0)	0.03
16	Monoglyceride lipase	33 708	64	13 (3)	7 (2)	0.46
17	Fructose-bisphosphate aldolase A	39 787	45	3 (1)	3 (1)	0.17
18	Creatine kinase M-type	43 246	36	25 (2)	10 (1)	0.16
19	Advanced glycosylation end product-specific receptor	42 984	19	2 (0)	1 (0)	0.08
20	Beta-enolase	47 337	31	9 (1)	8 (1)	0.07
21	Fatty acid-binding protein, epidermal	15 470	19	1 (1)	1 (1)	0.22
22	40S ribosomal protein SA	32 931	28	3 (1)	3 (1)	0.1
23	Myosin light chain 3	22 521	635	41 (30)	14 (11)	3.6
24	Serum albumin	70 700	302	25 (17)	12 (7)	0.44
25	Vimentin	53 712	24	1 (0)	1 (0)	0.06
26	Phosphoglycerate mutase 1	28 928	217	19 (11)	7 (4)	0.92
27	Adenylate kinase isoenzyme 1	21 640	49	21 (3)	8 (3)	0.78
28	Pyruvate dehydrogenase protein X component, mitochondrial	54 250	39	3 (2)	3 (2)	0.13
29	Myosin regulatory light chain 2, skeletal muscle isoform	19 057	44	18 (2)	4 (2)	0.38
30	Dynein heavy chain 12, axonemal	3 587 387	31	1 (1)	1 (1)	0.01

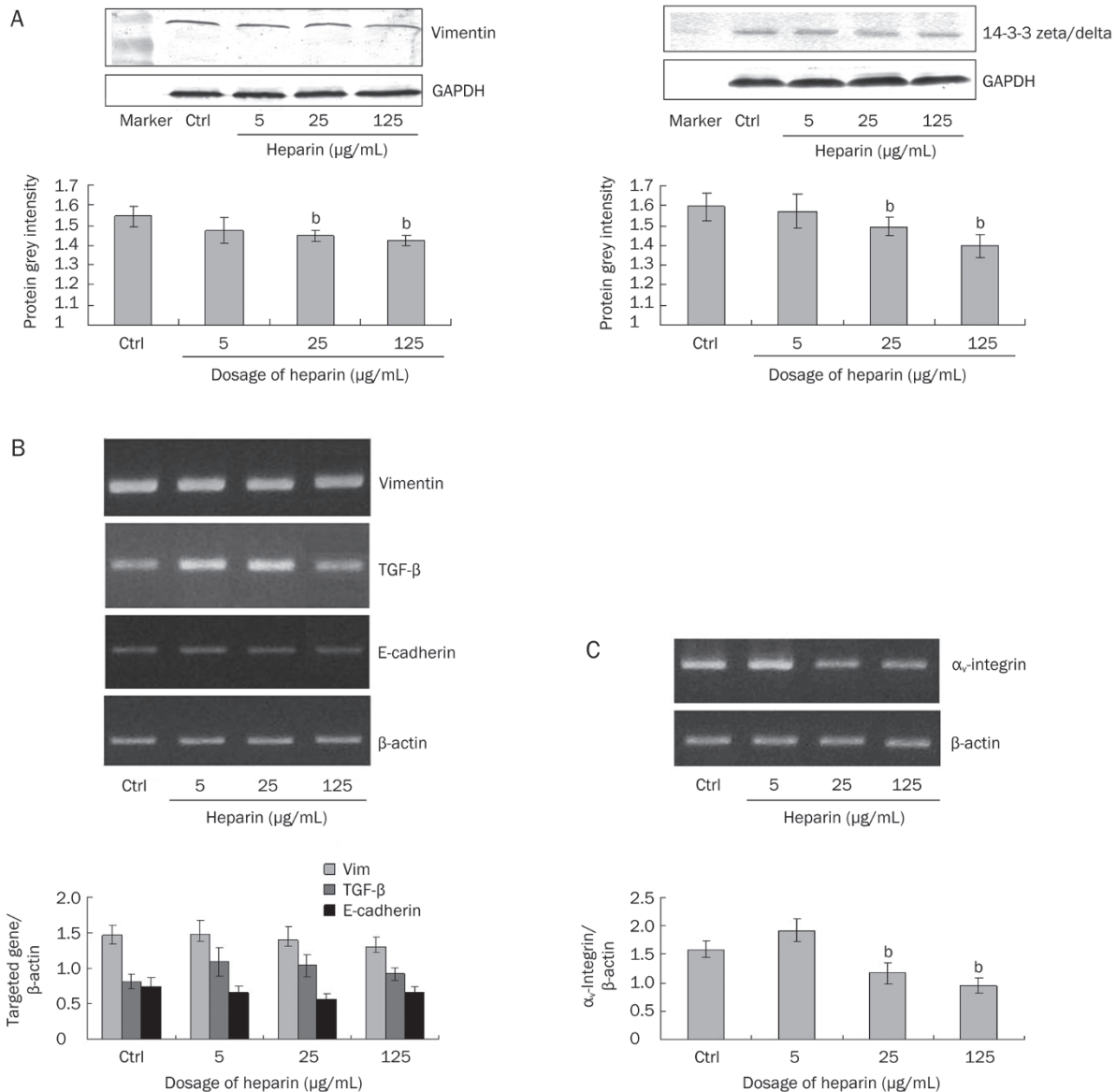


Figure 4. Effects of heparin on protein expression of vimentin and 14-3-3 zeta/delta (A) and mRNA expression of vimentin, TGF-β, E-cadherin, and α_v-integrin (B, C) in PC-3M cells. Mean ± SEM. *n* = 3. ^b*P* < 0.05 vs. the vehicle-treated control group. Each independent experiment was performed three times.

Discussion

In the experimental metastasis model, B16F10-luc-G5 tumor cells stably expressing firefly luciferase injected intravenously in the tail vein develop into pulmonary metastasis and are easily detected *in vivo* over time. We obtained results similar to that of others^[8–10] in that a single administration of heparin 30 min before injection of tumor cells into the tail vein could significantly inhibit this lung metastasis. In our study, with a second administration of heparin at 24 h after tumor cell injection, the lung metastasis could be significantly inhibited throughout the 14-day experimental period. APTT data showed that this injection of heparin was safe. As blood disorders (*ie*, low hematocrit) have been reported in cancer patients, we also analyzed hemorheological parameters in Balb/c nude mice

burdened with B16-F10-luc-G5 cells. Erythrocyte deformability and hematocrit were decreased, while the whole blood viscosity was increased in the model group compared to those of normal subjects^[11, 12]. The observation that heparin could maintain the normal levels of these blood parameters and also inhibit metastasis as mentioned above indicated that the influence of heparin on circulating cells was related to its inhibition of tumor development.

The effect of heparin on tumors includes interference with cancer-induced hypercoagulation, cancer cell proliferation, degradation of the extra-cellular matrix (involving the heparan sulfate chains of cell surface and extracellular matrix proteoglycans), angiogenesis, selectin-mediated binding of platelets and cancer cells, growth factors and their receptors, hepara-

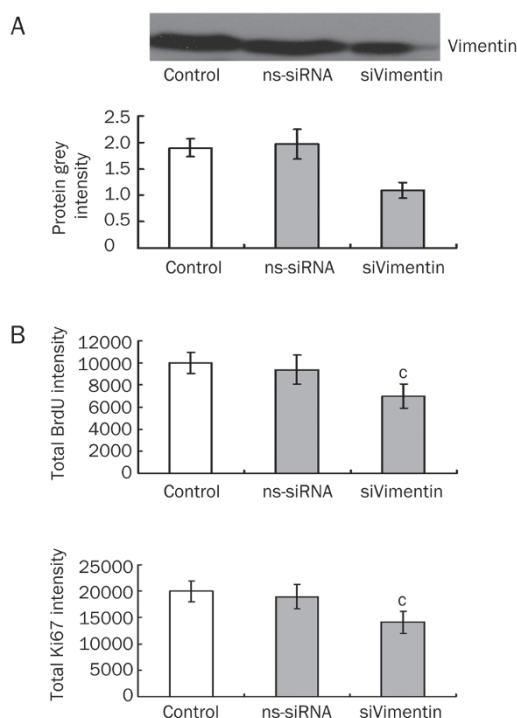


Figure 5. siRNA interferes with vimentin expression in PC-3M cells. Non-silencing siRNA (ns-siRNA) was used as a negative control. Vimentin-targeted siRNA (siVimentin) was transfected into PC-3M for 48 h; the total protein was extracted with protein lysis buffer and protein concentrations were measured using the Bradford protein assay. Cell lysates were analyzed by Western blotting (A). The effect of this vimentin knockdown on BrdU incorporation and Ki67 expression (B) in PC-3M cells. A total of 3000 cells were plated per well and incubated for 24 h. Mean \pm SEM. $n=6$. $^{\circ}P<0.01$ compared with control. Each independent experiment was performed three times.

nase, tumor progression, and metastasis^[13,14]. Heparin was proposed to have a role in maintaining the effects of chemotherapeutic drugs, as both UFH and LMWH have been shown to act as chemotherapy sensitizers^[4,5]. In our evaluation of the influence of heparin on tumor cell proliferation, cell cycle and apoptosis, we found that it could inhibit proliferation of PC-3M tumor cells and arrest them in the G_0/G_1 phase. Heparin has been reported to induce apoptosis in tumor cells mediated by caspase-3, caspase-8, Fas, and Bcl-2^[15]. In this study, we did not find a significant influence of heparin on tumor cell apoptosis, although there was a slight increase in number of apoptotic PC-3M cells treated with heparin (125 μ g/mL).

To gain a global overview of protein changes in response to heparin treatment, we utilized the 2-DE method to evaluate PC-3M cells and lungs of mice bearing B16-F10-luc-G5 cells. Our 2-DE analysis identified 60 different down-regulated proteins in PC-3M tumor cells and lungs after heparin treatment. The functions of those differentially expressed proteins are related to cell structure and movement (eg, fascin, transgelin, filamin, myosin, vimentin, dynein), cell growth and apoptosis (eg, anterior gradient protein 2, pyruvate kinase isozymes

M1/M2, enolase, 14-3-3 zeta/delta), energy metabolism (eg, adenylate kinase isoenzyme 1, ATP synthase subunit alpha, dihydrolipoyllysine-residue succinyltransferase component of 2-oxoglutarate dehydrogenase complex), nuclear activity regulation (eg, GTP-binding nuclear protein Ran) and several chaperones in the control of cell proliferation (eg, stress-70 protein, T-complex protein 1, heat shock protein HSP 90, heat shock protein 75 and endoplasmic).

After comparing the 2-DE results from PC-3M cells and lungs of mice burdened with B16-F10-luc-G5 cells, we found five protein spots which were identified in common: adenylate kinase isoenzyme 1, 14-3-3 protein zeta/delta, vimentin, phosphoglycerate mutase 1 and β -enolase.

Previously, based on the hypothesis that heparin regulates vimentin in the tumor-endothelium interaction and the finding of endothelial 2-DE experiment that vimentin expression altered greatly by low molecular weight heparin, we demonstrated that vimentin partly plays a role in the anti-metastatic effects of low molecular weight heparin^[16]. In the present study, we further analyzed and confirmed the down-regulated expression of vimentin, which was also one of the proteins influenced by heparin and identified in both the PC-3M cells and lungs of mice burdened with B16-F10-luc-G5 cells, along with 14-3-3 zeta/delta. The 14-3-3 zeta/delta belongs to a family of highly conserved proteins that play important roles in a wide range of cellular processes including apoptosis, cell cycle progression, and signal transduction. 14-3-3 proteins regulate the cell cycle and prevent apoptosis by controlling the nuclear and cytoplasmic distribution of signaling molecules with which they interact. In our pharmacodynamics studies about heparin on PC-3M tumor cells, we found that heparin have obviously inhibitory effects on tumor growth, proliferation and cell cycle. Additionally, the 14-3-3 dimer can bind to vimentin polypeptides and regulate Raf activation by EGF^[17], 14-3-3 protein plays an organizing role in the intermediate filament network^[18], and its overexpression has been found in multiple cancers. 14-3-3 zeta and delta both have been identified as biomarkers for poor prognosis, therapy and chemoresistance in multiple tumor types^[19,20]. Thus, vimentin and 14-3-3 are of interest as their protein expression levels were found to be significantly decreased by heparin in PC-3M cells. Our results of vimentin-targeted siRNA showed that partial knockdown of vimentin in PC-3M could reduce the ability of PC-3M cells proliferation. The inhibitory effects of heparin on structural organization of vimentin play an important role in its anti-tumor and anti-metastasis function. Meaningfully, activation of an Akt-14-3-3 zeta signaling pathway in promoting a multidrug-resistant phenotype has been associated with vimentin-dependent invasive behavior in diffuse large B-cell lymphoma cells^[21]. These proteins may account for the effect of heparin as a chemotherapy sensitizer, but further research on the role of 14-3-3 and vimentin in multi-drug resistance to anti-tumor agents should be undertaken.

In recent years, the cytoskeleton protein vimentin has gained attention for its roles in cell migration, adhesion, EMT, and signal transduction. In cancer-related studies, vimentin

has been found to be mainly involved in tumor mobility^[22, 23]. Vimentin has been shown to co-localize with $\alpha_v\beta_3$ -integrin (focal contacts)^[24]. Moreover, through integrin-linked kinase, integrin can regulate expression and function of vimentin. The levels of vimentin and integrin play a key role in tissue homeostasis as well, and their hyperexpression leads to tumorigenesis^[25, 26]. We detected and observed that the mRNA expression levels of α_v -integrin and vimentin could be mediated by heparin treatment.

In conclusion, our study has demonstrated multiple effects of heparin on tumors, consistent with previous studies that have identified heparin as an anti-cancer drug with diverse targets. These effects of heparin involve the inhibition of 14-3-3 zeta/delta, vimentin and α_v -integrin expression.

Acknowledgements

This work was supported by the National Natural Science Foundation of China (No 81020108031, 30572202, 30973558, 30772571, 30901815, 30901803), the Major Specialized Research Fund from the Ministry of Science and Technology in China (No 2009ZX09103-144), Research Fund from Ministry of Education of China (111 Projects No B07001) and Scientific Research Foundation for the Returned Overseas Chinese Scholars, State Education Ministry.

Author contribution

Yan PAN, Hong ZHOU, and Xue-jun LI designed research; Yan PAN, Li-jun ZHONG, Kui CHEN, Hao-peng YANG, Yilixiati XIAOKAITI, Aikebaier MAIMAITI, and Ling JIANG performed research; Yan PAN, Xin WANG, and Li-jun ZHONG analyzed data; Yan PAN and Xue-jun LI wrote the paper.

References

- Mandal AK, Lyden TW, Saklayen MG. Heparin lowers blood pressure biological and clinical perspectives. *Kidney Int* 1995; 47: 1017–24.
- Neison RM, Ceconi O, Roberts G, Aruffo A, Linhard RJ, Bcvilaqua MP. Heparin oligosaccharides bind L- and P-selection and inhibit acute inflammation. *Blood* 1993; 82: 3253–61.
- Li HL, Ye KH, Zhang HW, Luo YR, Ren XD, Xiong AH, et al. Effect of heparin on apoptosis in human nasopharyngeal carcinoma CNE2 cells. *Cell Res* 2001; 4: 311–5.
- Lebeau B, Chastang C, Brechot JM, Capron F, Dautzenberg B, Delaisements C, et al. Subcutaneous heparin treatment increases survival in small cell lung cancer. *Cancer* 1994; 1: 38–45.
- Altinbas M, Coskun HS, Er O, Ozkan M, Eser B, Unal A, et al. A randomized clinical trial of combination chemotherapy with and without low-molecular-weight heparin in small cell lung cancer. *J Thromb Haemost* 2004; 8: 1266–71.
- Niers TM, Klerk CP, DiNisio M, Van Noorden CJ, Büller HR, Reitsma PH, et al. Mechanisms of heparin induced anti-cancer activity in experimental cancer models. *Crit Rev Oncol Hematol* 2007; 3: 195–207.
- Pan Y, Iwata F, Wang D, Muraguchi M, Ooga K, Ohmoto Y, et al. Identification of aquaporin-5 and lipid rafts in human resting saliva and their release into cevimeline-stimulated saliva. *Biochim Biophys Acta* 2009; 1: 49–56.
- Boeryd B. Effect of heparin and plasminogen inhibitor (EACA) in brief and prolonged treatment on intravenously injected tumor cells. *Acta Pathol Microbiol Scand* 1966; 68: 347–54.
- Hagmar B, Boeryd B. Disseminating effect of heparin on experimental tumor metastases. *Pathol Eur* 1969; 4: 274–82.
- Maat B. Extrapulmonary colony formation after intravenous injection of tumor cells into heparin-treated animals. *Br J Cancer* 1978; 3: 369–76.
- Ramakrishnan S, Grebe R, Singh M, Schmid-Schönbein H. Evaluation of hemorheological risk factor profile in plasmacytoma patients. *Clin Hemorheol Microcirc* 1999; 20: 11–9.
- Rickles FR, Falanga A. Molecular basis for the relationship between thrombosis and cancer. *Thromb Res* 2001; 6: V215–24.
- Mousa SA, Petersen LJ. Anti-cancer properties of low-molecular-weight heparin: preclinical evidence. *Thromb Haemost* 2009; 102: 258–67.
- Casu B, Vlodavsky I, Sanderson RD. Non-anticoagulant heparins and inhibition of cancer. *Pathophysiol Haemost Thromb* 2008; 36: 195–203.
- Erduran E, Tekelioglu Y, Gedik Y, Bektaş I, Hacisalihoglu S. *In vitro* determination of the apoptotic effect of heparin on lymphoblasts using DNA analysis and measurements of Fas and Bcl-2 proteins by flow cytometry. *Pediatr Hematol Oncol* 2004; 5: 383–91.
- Pan Y, Lei TL, Teng B, Liu JH, Zhang JZ, An Y, et al. Role of vimentin in inhibitory effects of low molecular weight heparin on PC-3M adhesion to and migration through endothelium. *J Pharmacol Exp Ther* 2011; 339: 82–92.
- Tzivion G, Luo ZJ, Avruch J. Calyculin A-induced vimentin phosphorylation sequesters 14-3-3 and displaces other 14-3-3 partners *in vivo*. *J Biol Chem* 2000; 275: 29772–8.
- Satoh J, Yamamura T, Arima K. The 14-3-3 protein epsilon isoform expressed in reactive astrocytes in demyelinating lesions of multiple sclerosis binds to vimentin and glial fibrillary acidic protein in cultured human astrocytes. *Am J Pathol* 2004; 165: 577–92.
- Yang X, Cao W, Zhang L, Zhang W, Zhang X, Lin H. Targeting 14-3-3zeta in cancer therapy. *Cancer Gene Ther* 2012; 19: 153–9.
- Neal CL, Yu D. 14-3-3 ζ as a prognostic marker and therapeutic target for cancer. *Expert Opin Ther Targets* 2010; 14: 1343–54.
- Maxwell SA, Cherry EM, Bayless KJ. Akt, 14-3-3 ζ , and vimentin mediate a drug-resistant invasive phenotype in diffuse large B-cell lymphoma. *Leuk Lymphoma* 2011; 52: 849–64.
- Shirahata A, Sakata M, Sakuraba K, Goto T, Mizukami H, Saito M, et al. Vimentin methylation as a marker for advanced colorectal carcinoma. *Anticancer Res* 2009; 29: 279–81.
- Vora HH, Patel NA, Rajvik KN, Mehta SV, Brahmabhatt BV, Shah MJ, et al. Cytokeratin and vimentin expression in breast cancer. *Int J Biol Markers* 2009; 23: 38–46.
- Tsuruta D, Jones JC. The vimentin cytoskeleton regulates focal contact size and adhesion of endothelial cells subjected to shear stress. *J Cell Sci* 2003; 116: 4977–84.
- Zhang X, Fournier MV, Ware JL, Bissell MJ, Yacoub A, Zehner ZE. Inhibition of vimentin or beta1 integrin reverts morphology of prostate tumor cells grown in laminin-rich extracellular matrix gels and reduces tumor growth *in vivo*. *Mol Cancer Ther* 2009; 3: 499–508.
- Bhattacharya R, Gonzalez AM, Debiase PJ, Trejo HE, Goldman RD, Flitney FW, et al. Recruitment of vimentin to the cell surface by beta3 integrin and plectin mediates adhesion strength. *J Cell Sci* 2009; 122: 1390–400.